Application of Principles of Adaptive Control for Magnetic Levitation and Suspension Systems

1st Parichit Kumar (20736437)
Department of Mechanical and Mechatronics Engineering
University of Waterloo
Ontario, Canada
p43kumar@uwaterloo.ca

***Abstract*—The governing equation describing magnetic levitation tends to be non-linear. This paper compares the effects of inclusion of Adaptive Control principles to the conventional control strategies. It also covers the effect of linearization of a non-linear system. The Pole Placement Control strategy and the Sliding Mode Control strategy are covered here.**

***Index Terms*—Magnetic Levitation, Adaptive Control, Pole Placement, Sliding Mode**

I. Introduction

Principles of Magnetic Levitation have a wide array of applications. Magnetic levitation has proved to be relevant in fields like energy harvesting techniques [1], magnetically levitated trains [2], to manipulation of micro-robots [3] amongst many other fields.

Magnetic levitation and suspension techniques have a potential to be enable suspension of parts in the Additive Manufacturing industry as well. [4] depicts Boeing using the principles of Magnetic Levitation to suspend a part being manufactured. This technique enables multiple material jets to work in conjunction with one another to substantially decrease manufacturing time and increases the number of planes for material addition. This technique also bypasses the need for a substrate, i.e., the build surface to enable material addition [5]. As an initial step, a sphere of constant mass is suspended using the principles of magnetic levitation.

This paper deals with the development of different control strategies to successfully suspend the sphere of constant mass and comparing these control strategies and optimizing them through the principles of Adaptive Controls covered in [6].

II. Literature Review

Magnetic suspension and levitation techniques have been reviewed quite heavily over time. For instance, [7] deals with the development of the analytical model for the induced Eddy currents and the force generated as a consequence. It uses the principles of Faraday's law and Lorentz Law to develop the differential equations governing the system and solving these using the application of the appropriate boundary conditions and the principles of Orthogonality. The time varying magnetic field generated is a sinusoidal function given by $B_0 sin(\omega t)$ The final equation generated here is given by:

$$J_x = \Sigma \frac{\mu_m}{d} A_{nm} N_{nm} sin(\nu_n x) cos(\mu_m y) sin(\omega t)$$

$$J_y = -\Sigma \frac{\nu_n}{d} A_{nm} N_{nm} cos(\nu_n x) sin(\mu_m y) sin(\omega t)$$

where $N_{nm} = \frac{2}{\sqrt{ab}}$, $\nu_n = \frac{n\pi}{a}$, $\mu_m = \frac{m\pi}{b}$ and

$$A_{nm} = \frac{2k^2 B_0 d}{\mu_0 \sqrt{ab}} \frac{K(a,b,c) sin(\omega t)}{(\nu_n^2 + \mu_m^2) + k^2(1+gd) cos(\omega t)}$$

$$K(a,b) = \frac{[1 - cos(\nu_n a)][a - cos(\mu_m b)]}{\nu_n \mu_m}$$

The induced vector is then used to find the force generated.

[8] looks at the suspension of an Aluminum disk using the principles of magnetic levitation. Due to the high complexity of the analytical models developed, [8] uses a Simulation software (FEMM software) to generate the vertical force generated in the disk. The primary objective of the work conducted was to optimize the dimensions of the disk in consideration. An iterative methodology was implemented where simulations were conducted repeatedly until the peak force in the z-axis was obtained. The results of the simulations were then validated through experiments.

III. Theory

According to [9], Ampere's circuital law relates the integrated magnetic field around a closed loop to the electric current passing through the loop. It is governed by the following equation.

$$\nabla \times B = \mu_0 J$$

Faraday's Law states that the electromotive force around a closed path is equal to the negative of the time rate of change of the magnetic flux enclosed by the path [10]. This means that a current carrying conductor carrying a time varying current produces an induced EMF in another conductor that is governed by the equation:

$$E = -\frac{d\phi}{dt}$$

The induced EMF results in the generation of currents within the conductor. These are called Eddy Currents [11]. The induced Eddy currents interact with the magnetic field of the conductor carrying the time varying magnetic field to generate a force in the Z-axis. This force is used for the generation of the levitation force. The force generated is governed the principle of Lorentz Law and is given by the equation [12]:

$$F = qv + qv \times B$$

IV. Primary Analytical Model

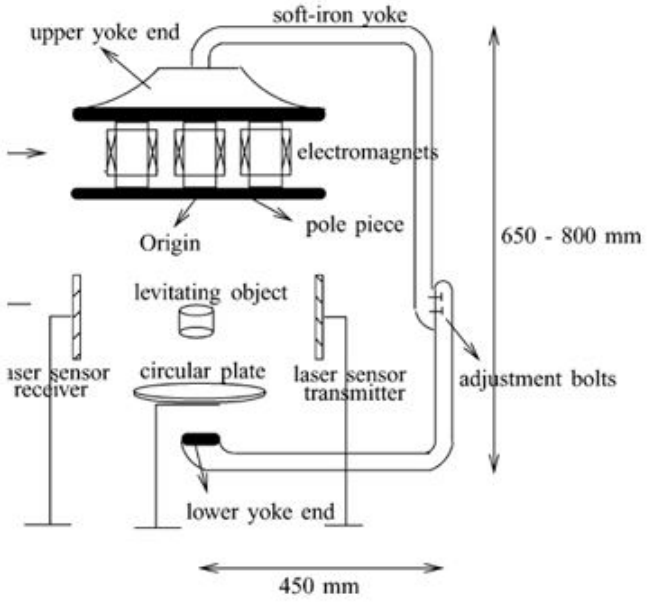

Fig. 1. Reference System obtained from [13]

Due to the complexity associated with the interaction between the permanent and electro-magnet system, the governing analytical models derived theoretically are very complex. However, [13] depicts the use of experimental methods to derive a governing equation depicting the interaction between the permanent magnets and electro-magnet systems. The system is depicted in figure 1. This is given by the following equation:

$$m\frac{d^2h}{dt^2} = F_{lev} - mg \tag{1}$$

From experiments conducted, the value of F_{lev} is given by:

$$F_{lev} = \alpha Ih + \beta h \tag{2}$$

Substituting 2 in 1, the following is obtained:

$$m\frac{d^2h}{dt^2} = \alpha Ih + \beta h - mg \tag{3}$$

Equation 3 is used for modelling the system and generating the control strategies.

The system would accept a time varying current as an input. This time varying current will result in the generation of a time varying magnetic field which would then interact with the object being levitated to generate a stabilizing force. This current would be adjusted to enable effective magnetic levitation. The primary parameter tracked within the system is the position of the object being levitated. The position is read using a position sensor and is fed back to the controller to enable a feedback mechanism.

V. Principle of Adaptive Control

The system modelled in this paper assumes that the plant parameters are not constant as time progresses. These plant estimates are a function of time. This is specially useful in the system model here since the governing equation obtained is a function of experimental constants. Thus, through the principles of adaptive control, these constants are estimated at each iteration to optimize the control strategy.

A. Estimation Model

Rewriting equation 3 to put the unknown plant parameters on the RHS and the known and measurable parameters on the LHS, the following is obtained:

$$ms^2h - mg = \alpha Ih + \beta h \tag{4}$$

Since the acceleration is not available for measurement, a suitable filter is applied. The filter is given by:

$$\frac{1}{\Lambda(s)} = \frac{1}{(s+1)^2} \tag{5}$$

Multiplying the filter from 5 on both sides of 4:

$$m\frac{s^2h}{(s+1)^2} - \frac{mg}{(s+1)^2} = \alpha\frac{Ih}{(s+1)^2} + \beta\frac{I}{(s+1)^2} \tag{6}$$

The estimation model is given by:

$$z = \theta^{*T}\phi$$

where

$$z = m\frac{s^2h}{(s+1)^2} - \frac{mg}{(s+1)^2}$$

$$\theta^{*T} = [\alpha, \beta]$$

$$\phi = [Ih, I]$$

It should be noted that θ^* is constant over time. ϕ is available for measurement at every iteration of time. It is also assumed that the mass is constant.

B. Error Model

The estimation error is the difference between the output of the simple parametric model computed (z) and the estimated parametric model ($\hat{z}$) resulting from the adaptive control algorithm. Essentially, θ^* is replaced with the estimated $\theta(t)$ and the difference between the two is the estimation error. It is given by:

$$\epsilon = \frac{z - \hat{z}}{m_s^2}$$

where m_s^2 is the normalized signal that ensures that $\frac{\phi}{m_s^2}$ is bounded. Here, $m_s^2 = 1 + \alpha\phi^T\phi$, where α ¿0.

C. Adaptive Law

1) Gradient Law: The governing equation for the Gradient based adaptive law is given by:

$$\dot{\theta} = \Gamma\epsilon(t)\phi(t)$$

where Γ is a symmetric, positive definite, 2x2 matrix where $\Gamma = \Gamma^T > 0$. The value of the Γ matrix was selected through trial and error.

Stability: If the input u is sufficiently rich (of order n), then the estimated plant $\theta(t)$ will converge to θ^* as time tends to infinity.

2) Least Square: The governing equation for the least square adaptive algorithm is given by:

$$\dot{\theta} = P\epsilon(t)\phi(t)$$

$$\dot{P} = \beta P - P\frac{\phi\phi^T}{m_s^2}P$$

β is the forgetting factor.

Stability: If $\frac{\phi}{m_s^2}$ is Persistently Excited, then $\theta(t)$ converges to θ^* as time tends to infinity.

VI. Control Strategies

In this section, different control algorithms were implemented to test their viability. During implementation here, it is assumed that all the plant parameters are known. The two control strategies implemented are:

1) Pole Placement Control (PPC)
2) Sliding Mode Control (SMC)

A. Pole Placement Control

In PPC, the non-linear governing equation is linearized and the control strategy is implemented. Following the computation of the control input, a linearization compensation block is added and the new input is fed into the plant. The control diagram for the same is given by fig. 2.

Substituting $y = e + y_d$, where e is the error and y_d is the desired output in equation 3, the following governing equation is obtained:

$$s^2 e = \frac{\alpha(e + y_d) + \beta}{m}u \tag{7}$$

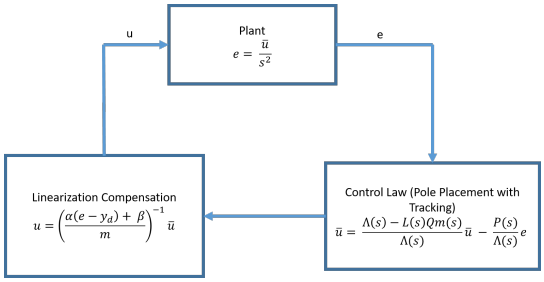

Fig. 2. Control Diagram for PPC

Assuming the input $\bar{u}$ as follows:

$$\bar{u} = \frac{\alpha(e + y_d) + \beta}{m}$$

Thus, the governing control equation is given by:

$$e = \frac{\bar{u}}{s^2}$$

The control task is to push the error e to 0. The poles of the system are placed at -10 to ensure a stable system.

Thus, the control law is given by:

$$u = \frac{-39s + 1}{s^2 + s + 1}u + \frac{600s^2 + 4000s + 10000}{s^2 + s + 1} \tag{8}$$

The control strategy described in fig. 2 and equation 10 was implemented using Simulink and the plot obtained is shown in figure 3.

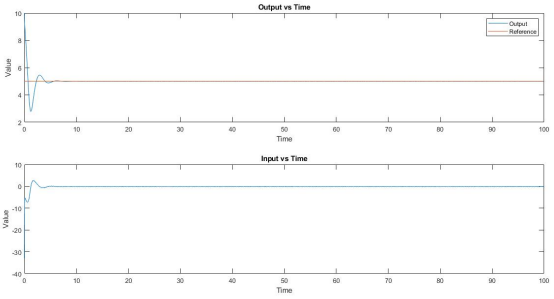

Fig. 3. Simulation Plots for PPC

B. Sliding Mode Control

The Sliding Mode Controller is a control strategy implemented for non-linear systems. The general form of these systems if given by:

$$\dot{X} = F(X) + G(X)u$$

The governing equation in equation 3 is a non-linear equation.

$$s^2 e = \frac{\alpha(e + y_d) + \beta}{m}u \tag{9}$$

Here, $X = e$, $F(X) = 0$ and $G(X) = \frac{\alpha(e+y_d)+\beta}{m}$. The control law for SMC is given by:

$$u = G(x)^{-1}(F(X) + \ddot{y_d} - S - ksgn(S))$$

where $S = \dot{e} + \lambda e$ which is the sliding condition. λ is a constant. In order to create a boundary on the sliding surface, the sgn function in imposed on the same.

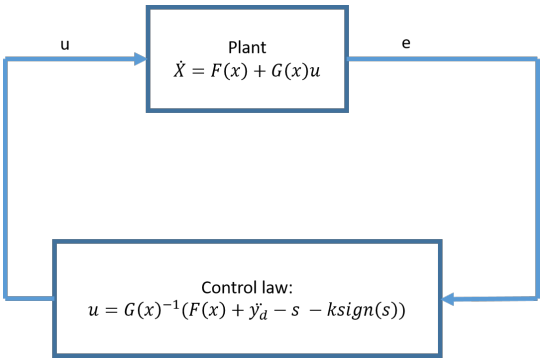

Fig. 4. Control Diagram for SMC

$$sgn(S) = \begin{cases} -1 & S \leq -\hat{\epsilon} \\ \frac{S}{\hat{\epsilon}} & -\hat{\epsilon} \leq S \leq \hat{\epsilon} \\ 1 & \hat{\epsilon} \leq S \end{cases}$$

The control objective here is to push the error (e) to 0. Thus, the control diagram for the SMC is given by figure 4 was simulated in Simulink. The plots obtained are shown in figure 5.

VII. Implementation of Adaptive Control

The principles of adaptive control described in section V are applied to the control strategies described in section VI-A. Here, the plant estimates generated from the adaptive control algorithm are fed into the control law and the new input is fed into the plant to obtain the output.

A. Adaptive Pole Placement Control

Since the plant parameters obtained from the adaptive law are only fed into the linearization compensation block, the implementation of the control algorithm remains the same here. The plant estimates are fed into the linearization block and the input obtained is fed into the plant.

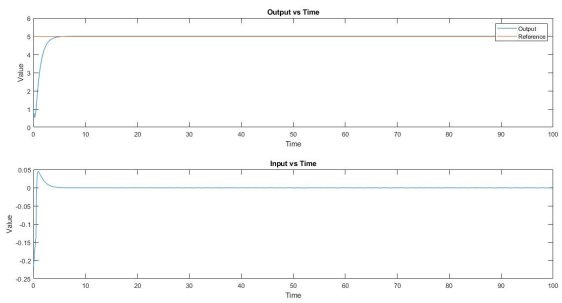

Fig. 5. Simulation Plots for SMC

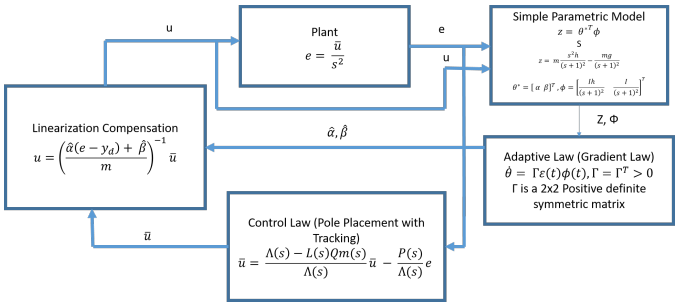

Fig. 6. Control Diagram for Adaptive PPC

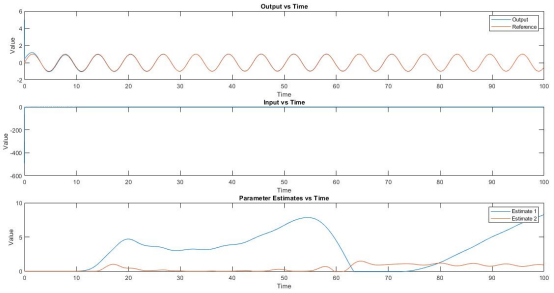

Fig. 7. Adaptive PPC for a Sinusoidal y_d

The control diagram is shown in figure 6.
The governing control law is given by:

$$u = \frac{-39s + 1}{s^2 + s + 1}u + \frac{600s^2 + 4000s + 10000}{s^2 + s + 1} \tag{10}$$

The linearization compensation is given by the following:

$$\bar{u} = \frac{\hat{\alpha}(e + y_d) + \hat{\beta}}{m}$$

$\hat{\alpha}$ and $\hat{\beta}$ are the plant estimates obtained through the implementation of the principles of adaptive control. The control law described in the figure 6 was implemented in Simulink. Two different desired output states were implemented. For $y_d = (5mm)$, the plots obtained are shown in figure 8. For $y_d = sin(t)$, the plots obtained are shown in figure 7.

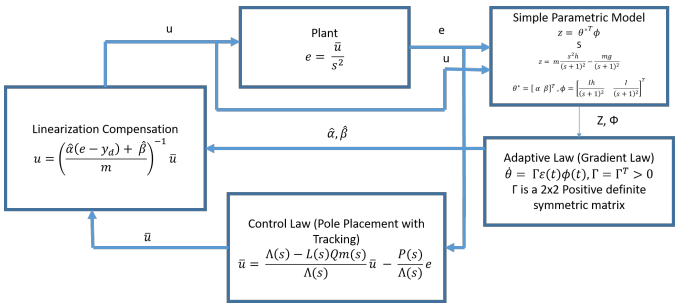

Fig. 8. Adaptive PPC for a Constant y_d

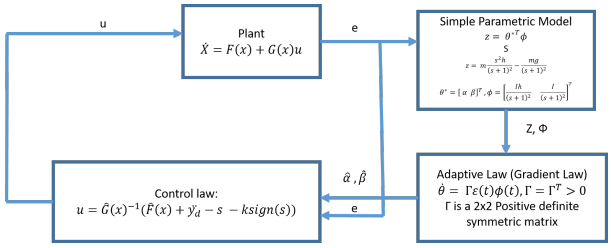

Fig. 9. Control Block Diagram for Adaptive SMC

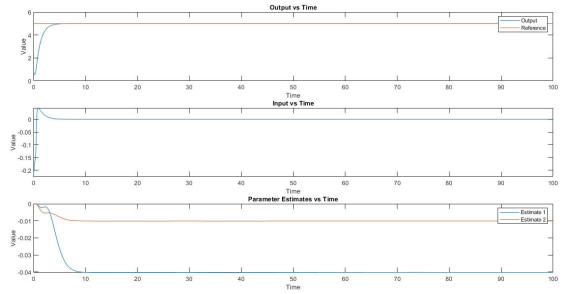

Fig. 10. Simulation Plots for Adaptive SMC for $y_d = 5mm$

B. Adaptive Sliding Mode Controller

As opposed to the APPC, the plant estimates obtained from the principles of adaptive control shown in section V are fed into the control law described in section VI-B. Thus, the revised control diagram for the system is shown in figure 9.

Thus, the revised control law is given by:

$$u = \hat{G}(x)^{-1}(\hat{F}(X) + \ddot{y_d} - S - ksgn(S))$$

Where, $\hat{F}X) = 0$ and $\hat{G}(X) = \frac{\hat{\alpha}(e+y_d)+\hat{\beta}}{m}$. $\hat{\alpha}$ and $\hat{\beta}$ are the plant estimates obtained through the implementation of the principles of adaptive control.

The control law described in the figure **??** was implemented in Simulink. Two different desired output states were implemented. For $y_d = 5mm$, the plots obtained are shown in figure 10. For $y_d = sin(t)$, the plots obtained are shown in figure 11.

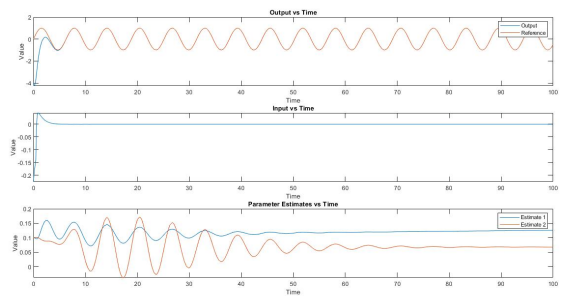

Fig. 11. Simulation Plots for Adaptive SMC for $y_d = sin(t)$

VIII. Results and Discussions

A. Effect of Linearization

A comparison between figure 3 and figure 5 shows the effect of linearization to the non-linear system. Considering the linearized system with Pole Placement Control, it can be seen from figure 3 that there is a very heavy overshoot of about 4 mm from the desired state. Due to the relatively compact space available for magnetic levitation, the overshoot might result in undesired complications.

For the non-linear control system utilizing Sliding Mode Controller, figure 5 shows little to no overshoot. This would be ideal since the controller achieves the control objective effectively and minimizes the probability of complications.

B. Effects of the Principles of Adaptive Control

Figures 3 and 7 are compared to discuss the effects of the inclusion of adaptive controls principles. As it can be seen from figure 8, the overshoot observed in figure 3 in the conventional Pole Placement Controller have been minimized quite significantly. This shows that the controller achieves its control objective more effectively. It should also be noted that the Adaptive Pole Placement Controller stabilizes in lesser time when compared to its PPC counterpart. Thus, the effects of the inclusion of Adaptive control principles are heavily emphasized.

To discuss the effectiveness of the principles of adaptive controls for Sliding Mode controller, figures 5 and 10 are compared. The adaptive SMC does not have a considerably improved performance (shown in figure 10) when compared its conventional SMC counterpart (shown in figure 5). Providing a time-varying desired state output also does not depict a clear improvement in performance.

C. Stabilization of the Plant Parameters

Based on the principles described in [6], if the input to the plant is Persistently Excited (PE), then estimated plant parameters $\theta(t)$ converge to constant plant parameter θ^* as time tends to infinity. A vector is defined as PE if it satisfies the following condition:

$$\int_t^{t+T_0} \phi(\tau)\phi^T(\tau)d\tau \geq \alpha_0 T_0 I$$

For some $\alpha_0 > 0$, $T_0 > 0$ $\forall$t≥ 0

From figures 10 and 6, it can be seen that the input stabilizes to zero. Thus, the input to the plant is not PE. Thus, the plant parameter do not stabilize to the expected value.

IX. Conclusion

Through the work depicted in this paper, it is evident that the use of Adaptive control principles in the control strategies results in improved system performances. The system stabilizes quickly and the reduces the degree of overshoot. The performance of the system is optimized for a time-varying desired state as well. The work also shows that the effects of linearization of the governing plant equation

does not drastically diminish the system performance. Thus, linearization and subsequent incorporation of the principles of adaptive controls can result in a high-performing system.

X. Future Scope of Work

Following the work conducted in this paper, the next steps of implementation are shown as follows:

1) The mass of the system (a plant parameter) should also be considered to be time-varying. Since there is material addition at every iteration in an Additive Manufacturing environment, the mass would need to be updates at every step and the control law would need to update the system input accordingly.
2) The system and the governing principles must also include the principle forces generated during the material addition phase. This can include principles such as nozzle jet forces, effects of accumulation of nucleus mass amongst others.
3) Noise can be added to the measurement of all measurable quantities (distance between the part and the Magnets and coil system). This implies that the sensor outputs are relatively flawed. This would mimic the real world system more closely.

XI. Acknowledgements

The work conducted in this paper was a part of the course ME-780: Adaptive Controls in Winter 2019. The work was conducted under the supervision of Dr. Baris Fidan.

References

[1] B. Mann and N. Sims, Energy harvesting from the nonlinear oscillations of magnetic levitation, Journal of Sound and Vibration, vol. 319, no. 1-2, pp. 515530, 2009.
[2] Lee, Hyung-Woo, et al. Review of Maglev Train Technologies. IEEE Transactions on Magnetics, vol. 42, no. 7, 2006, pp. 19171925., doi:10.1109/tmag.2006.875842.
[3] Shameli, Ehsan, et al. Nonlinear Controller Design for a Magnetic Levitation Device. Microsystem Technologies, vol. 13, no. 8-10, 2006, pp. 831835., doi:10.1007/s00542-006-0284-y.
[4] W. A. Harkness and J. H. Goldschmid , Free-Form Spatial 3-D Printing Using Part Levitation, 04-Feb-2016.
[5] J. Meyer, Substrate for additive manufacturing, 26-Sep-2013.
[6] P. A. Ioannou and Fidan Baris, Adaptive control tutorial. Philadelphia: Society for Industrial and Applied Mathematics, 2006.
[7] G. Sinha and S. S. Prabhu, Analytical model for estimation of eddy current and power loss in conducting plate and its application, Physical Review Special Topics - Accelerators and Beams, vol. 14, no. 6, 2011
[8] F. Ghayoor and A. Swanson, Modelling and analysis of electrodynamic suspension of an aluminium disc as a complex engineering problem, International Journal of Electrical Engineering Education, vol. 55, no. 2, pp. 91108, 2018.
[9] J. C. Maxwell, On Physical Lines of Force,The Scientific Papers of James Clerk Maxwell, pp. 451513.
[10] Sadiku, M. N. O. (2007). Elements of Electromagnetics (4th ed.). New York & Oxford: Oxford University Press. p. 386. ISBN 0-19-530048-3.
[11] Israel D. Vagner; B.I. Lembrikov; Peter Rudolf Wyder (17 November 2003). Electrodynamics of Magnetoactive Media. Springer Science Business Media. pp.73.ISBN978-3-540-43694-2
[12] I. D. Vagner, B. I. Lembrikov, and P. Wyder, Electrodynamics of Magnetoactive Media,Springer Series in Solid-State Sciences, 2004.
[13] C. Elbuken, E. Shameli and M. Khamesee, ”Modeling and Analysis of Eddy-Current Damping for High-Precision Magnetic Levitation of a Small Magnet”, IEEE Transactions on Magnetics, vol. 43, no. 1, pp. 26-32, 2007. Available: 10.1109/tmag.2006.885859